Protocols for optimal readout of qubits using a continuous quantum nondemolition measurement

Jay Gambetta,[1] W. A. Braff,[1] A. Wallraff,[1,2] S. M. Girvin,[1] and R. J. Schoelkopf[1]
[1]*Department of Applied Physics and Physics, Yale University, New Haven, Connecticut 06520, USA*
[2]*Department of Physics, ETH Zurich, CH-8093 Zurich, Switzerland*
(Received 4 January 2007; published 24 July 2007)

We study how the spontaneous relaxation of a qubit affects a continuous quantum nondemolition measurement of the initial state of the qubit. Given some noisy measurement record Ψ, we seek an estimate of whether the qubit was initially in the ground or excited state. We investigate four different measurement protocols, three of which use a linear filter (with different weighting factors) and a fourth which uses a full nonlinear filter that gives the theoretically optimal estimate of the initial state of the qubit. We find that relaxation of the qubit at rate $1/T_1$ strongly influences the fidelity of any measurement protocol. To avoid errors due to this decay, the measurement must be completed in a time that decrease linearly with the desired fidelity while maintaining an adequate signal to noise ratio. We find that for the nonlinear filter the predicted fidelity, as expected, is always better than the linear filters and that the fidelity is a monotone increasing function of the measurement time. For example, to achieve a fidelity of 90%, the box car linear filter requires a signal to noise ratio of $\sim$30 in a time T_1, whereas the nonlinear filter only requires a signal to noise ratio of $\sim$18.

DOI: 10.1103/PhysRevA.76.012325 PACS number(s): 03.67.Lx, 42.50.Lc, 03.65.Yz

I. INTRODUCTION

In this paper we consider the following problem. Given a qubit initially either in the ground or excited state with finite lifetime T_1, how can we best make use of a continuous-in-time noisy quantum nondemolition (QND) measurement to optimally estimate the *initial* state (ground or excited) of the qubit? A number of authors have previously considered the related problem of optimal estimation of the *present* state of the qubit based on the past and current measurement record [1–6], but, to the best of our knowledge, the problem we consider here has not been previously studied.

QND measurements play a central role in the theory and practical implementation of quantum measurements [7]. In a QND measurement, the interaction term in the Hamiltonian coupling the system to the measuring apparatus commutes with the quantity being measured, so that this quantity is a constant of the motion. This does *not* imply that the quantum state of the system is totally unaffected, but it does imply that the measurement is *repeatable*. For example, a Stern-Gerlach measurement of $\hat{\sigma}_z$ for a spin-1/2 particle initially prepared in an eigenstate of $\hat{\sigma}_x$ will randomly yield the results +1 and −1 with equal probability. However, all subsequent measurements of $\hat{\sigma}_z$ will yield exactly the same result as the initial measurement.

The fact that QND measurements are repeatable is of fundamental practical importance in overcoming detector inefficiencies. A prototypical example is the electron-shelving technique [8,9] used to measure trapped ions. A related technique is used in present implementations of ion-trap based quantum computation. Here the (extremely long-lived) hyperfine state of an ion is read out via state-dependent optical fluorescence. With properly chosen circular polarization of the exciting laser, only one hyperfine state fluoresces and the transition is cycling; that is, after fluorescence the ion almost always returns to the same state it was in prior to absorbing the exciting photon. Hence the measurement is QND. Typical experimental parameters [10] allow the cycling transition to produce $N\sim 10^6$ fluorescence photons. Given the photomultiplier quantum efficiency and typically small solid angle coverage, only a very small number $\bar{n}_{\mathrm{d}}$ will be detected on average. The probability of getting zero detections (ignoring dark counts for simplicity) and hence misidentifying the hyperfine state is $P(0)=e^{-\bar{n}_d}$. Even for a very poor overall detection efficiency of only 10^{-5}, we still have $\bar{n}_d=10$ and nearly perfect fidelity $F=1-P(0)\sim 0.999\,955$. It is important to note that the total time available for measurement is not limited by the phase coherence time (T_2) of the qubit or by the measurement-induced dephasing [3,4,11,12], but rather only by the rate at which the qubit makes real transitions between measurement ($\hat{\sigma}_z$) eigenstates. In a perfect QND measurement there is no measurement-induced state mixing [4] and the relaxation rate $1/T_1$ is unaffected by the measurement process.

The ability to read out a qubit with high fidelity is of central importance to the successful construction of a quantum computer [13]. In order to successfully measure a qubit, its quantum state must be mapped into a piece of classical information by measuring the relative occupation of its two states with the highest possible fidelity. Possible qubit implementations include superconducting circuits, silicon based electron and nuclear spins, and trapped ions, among others [14–23]. In order for qubits prepared in different states to be distinguishable, the measurement must be completed before the excited qubits decay [4,24]. Many atomic qubits have sufficiently long lifetimes so that relaxation is not a major concern [14,16,20], but most solid state qubits have lifetimes on the order of microseconds or less, and spontaneous relaxation plays a significant role in the measurement. The qubit relaxation affects different measurement schemes differently, but in all cases, it can limit the maximum fidelity.

Although the behavior of a qubit during continuous measurement has been studied using Monte Carlo simulations [2–6], no attempt has been made to derive an analytical expression for the probability distribution of the *initial* state or to study how spontaneous emission impacts the measurement

fidelity. This is at least partially because there exist very few high fidelity continuous QND measurements, and even fewer that operate in a regime where qubit relaxation is a limiting factor. With the application of low temperature amplifiers, high fidelity (though not necessarily weak continuous) measurements of superconducting qubits are now becoming feasible [19,23,25–32]. These measurements have found asymmetries between the probability distributions for the integrated signal corresponding to the ground and excited states, but could not accurately predict them.

Here we find that when we use a measurement protocol that only records the integrated signal, the qubit relaxation induces asymmetry in the probability distributions, and that with a sufficiently precise detector, the distributions become distinctly non-Gaussian. Unlike measurement of a perfect (i.e., nondecaying) qubit, where fidelity is always improved by a longer measurement, we show that there is some optimal measurement fidelity that depends on the signal to noise ratio (r_{sn}) of the detector and the filter used. The first filter we consider is the linear box car filter and optimize over the integrated time t_{f}. Choosing a longer or shorter integration time will lower the fidelity of the measurement. Next we show that by choosing a filter that gives exponentially less importance to results at later times slightly increases the fidelity. We then numerically find the optimal linear filter and compare these linear filters to a nonlinear filter that yields the theoretically optimal estimate of the initial state of the qubit given some measurement record Ψ. We find that we can reach the same fidelity as the linear filters at a substantially lower r_{sn}. Furthermore, due to the nature of the updating protocol, the fidelity is a nondecreasing function of the measurement time. In summary, in this paper we determine the optimal measurement fidelity given four measurement protocols for continuous measurement experiments currently being performed, and also provides a guideline for the necessary detector signal to noise ratio in order to reach a particular desired fidelity in future experiments.

There are two major ways of measuring qubits. The first method is a latching measurement, for example by having the qubit state modify the switching current (or state) of an adjacent Josephson junction [28,29] or the bifurcation point of the nonlinear Josephson plasma oscillation [30–32]. In such latching measurements, the qubit is measured very quickly with very high signal to noise, and after only a short waiting time [15,17,28,32]. Some versions of such strong measurements can in principle be QND [32]. The second method is to perform a sequence of repeated or weak continuous quantum nondemolition (QND) measurements, which each leave the populations of the qubit unchanged. Several recent experiments with solid-state qubits [23,33,34], have used continuous QND measurement schemes in which the qubit lifetime imposes the main limitation on the measurement fidelity, for which the analysis of this paper should apply.

It is not just continuous measurements that are affected by qubit relaxation. For example, consider an idealized latching measurement scheme where a qubit is prepared in an eigenstate, but there is some finite arming time t_{arm} before a perfect measurement is made. In this case, a qubit prepared in the ground state will always be measured correctly, but a qubit prepared in the excited state may have decayed during t_{arm} and be misidentified. Thus if t_{arm} is not infinitesimally small, the qubit lifetime places a limit on fidelity even with a perfect detector.

II. QUBIT WITH INFINITE LIFETIME

It is worthwhile to first consider the case when the qubit cannot relax from the state it is initially prepared in, so it is "fixed" for all time. This allows us to formalize our intuitive understanding of a general continuous measurement and to give us a result against which we can compare the finite lifetime case. We consider the measurement of a qubit with two states $|+\rangle$ (excited) and $|-\rangle$ (ground) and assume that the measurement result is given by the actual value of the qubit state plus Gaussian noise. This assumption is justified for example in the current circuit quantum electrodynamic experiments [11,12,22,23] in which a cavity is dispersively coupled to the qubit (no energy is exchanged between the cavity and the qubit). A homodyne measurement on the cavity output will reveal the cavity state (which is proportional to $\hat{\sigma}_z$) plus Gaussian noise [12,21]. This Gaussian noise will be at least the photon shot noise but in present experiments it is dominated by the following amplifier. In other words, the measurement is faithful and given that the system is in state $i=\pm 1$ our detector for a time interval $d\tau$ outputs $\psi(\tau)$ with statistics

$$P(\psi|i) = \sqrt{\frac{d\tau\, r_{\mathrm{sn}}}{2\pi}} \exp[-(\psi - i)^2 d\tau\, r_{\mathrm{sn}}/2]. \tag{2.1}$$

For convenience we have also introduced a dimensionless time $\tau = t/T_1$ where T_1 is an arbitrary but finite number, that will become the relaxation lifetime when we treat the finite lifetime case. Here r_{sn} is the ratio of integrated signal power to noise power. It is linear in the integration time and we will adopt the convention of specifying the r_{sn} as that achieved after integrating for time T_1.

From this distribution we can write $\psi(\tau)$ in terms of the Wiener increment $dW(\tau)$ [35] as

$$\psi(\tau)d\tau = i_{\pm}(\tau)d\tau + \sqrt{r_{\mathrm{sn}}^{-1}}dW(\tau). \tag{2.2}$$

Here we have introduced the subscript $\pm$ to indicate a possible realization of the dynamics of the qubit given the initial condition ± 1. For this case the qubit can be initialized in either state, but because it has an infinite lifetime, it is fixed in whatever state it starts in for the duration of the measurement. That is, $i_{\pm}(\tau) = \pm 1$.

We define our measurement signal s as the output of the detector integrated over time τ_f

$$s = \int_0^{\tau_f} d\tau\, \psi(\tau). \tag{2.3}$$

Formally we are restricting ourselves here to a simple box car linear filter which uniformly weights the measurement record $\psi(\tau)$ in the interval $0 < \tau < \tau_f$. Using Eq. (2.2) it is simple to carry out the above integral and rewrite the measurement signal as $s_{\pm}(\tau_f) = \pm\tau_f + X_G[0, \sigma^2]$ where $X_G[0, \sigma^2]$ is

TABLE I. The required minimum signal to noise ratio r_{sn} after T_1 and the optimal measurement time τ_{opt} for a continuous measurement of a qubit with infinite lifetime ($r_{sn(fixed)}$), a simple box car linear filter ($r_{sn(BC)}$), an exponentially decaying linear filter ($r_{sn(exp)}$), the optimal linear filter ($r_{sn(OL)}$), and a nonlinear Bayesian filter ($r_{sn(NL)}$). The last column is the maximum allowed waiting time τ_{arm} for an idealized latching (instantaneous) measurement with infinite signal to noise performed after time τ_{arm} in order to achieve the desired fidelity F.

F	$r_{sn(fixed)}$	$r_{sn(BC)}(\tau_{opt})$	$r_{sn(exp)}(\tau_{opt})$	$r_{sn(OL)}$	$r_{sn(NL)}$	τ_{arm}
50%	0.50	1.47(0.82)	1.23(1.59)	1.17	1.1	0.7
67%	1.0	4.05(0.55)	3.58(0.75)	3.10	2.9	0.40
90%	2.7	29.9(0.17)	28.7(0.18)	22.1	18.	0.11
95%	3.8	77.3(0.087)	75.7(0.090)	55.9	48.	0.05
99%	6.7	574.(0.018)	572.(0.018)	420	269.	0.01

a Gaussian random variable of mean 0 and standard deviation $\sigma=\sqrt{\tau_f/R^{(S/N)}}$. The signals then follow the familiar Gaussian distributions

$$P_{\pm}^{\text{fixed}}(s)=\frac{1}{\sigma\sqrt{2\pi}}e^{-(s\mp\tau_f)^2/(2\sigma^2)}. \tag{2.4}$$

Because these distributions are symmetric about $s=0$, the most obvious analysis is to set a signal threshold $\nu_{th}=0$ and call every measurement with $s>\nu_{th}$ a $(+1)$ state, and every measurement with $s<\nu_{th}$ a (-1) state. Calculation of fidelity in this case is accomplished using the definition

$$F\equiv 1-\int_{-\infty}^{\nu_{th}} ds\, P_+(s)-\int_{\nu_{th}}^{\infty} ds\, P_-(s). \tag{2.5}$$

For the case of infinite qubit lifetime we have the simple result

$$F=\text{erf}\left(\sqrt{\frac{\tau_f r_{sn}}{2}}\right). \tag{2.6}$$

A fidelity of zero corresponds to a completely random measurement that extracts no information, a fidelity of one corresponds to a perfect faithful measurement, and in between the measurement conveys varying degrees of certainty. As τ_f becomes large, Eq. (2.5) predicts that the fidelity rapidly approaches unity. Higher r_{sn} serves to speed up the convergence, but as long as r_{sn} is non zero, any desired fidelity is attainable simply by measuring the qubit for long enough. In Table I, the required $r_{sn(fixed)}$ is listed in order to achieve a given fidelity within T_1. Note the same results for the fidelity would be obtained if we used the optimal nonlinear filter of Sec. VI. That is, for a qubit with infinite lifetime the simple box car filter is equivalent to the optimal nonlinear filter, it is only when we include relaxation this is not the case. This will be discussed in detail in the next four sections.

III. BOX CAR LINEAR FILTER

A. Probability distributions for QND measurement

Here we consider the same measurement protocol as in Sec. II, however unlike a qubit with infinite lifetime, where both states behave similarly, a qubit with a finite lifetime has a fundamental asymmetry in how the excited and ground states behave. We assume (in our model) that the excited state decays at rate $1/T_1$ but the transition rate upward out of the ground state is zero. A qubit prepared in the ground state will never experience any excitations, so it can be treated much the same as the fixed qubit discussed above and hence $P_-(s)=P_-^{\text{fixed}}(s)$. By contrast, an initially excited qubit will produce an ensemble averaged output which will decay exponentially with characteristic dimensionless time $\tau_1\equiv 1$. Although most qubits dephase in some shorter dimensionless time τ_2, our only concern here is the relative population of the two qubit states, so we are not limited by decoherence of the qubit. For a single qubit, this translates into a single, abrupt relaxation of the qubit at some dimensionless time τ_d that is exponentially distributed with mean dimensionless time 1, $P(\tau_d)=\exp(-\tau_d)$. That is, if the qubit was initially in the excited state then $i_{\pm}(\tau)$ would obey

$$i_{\pm}(\tau)=\theta(\tau_d-\tau)-\theta(\tau-\tau_d). \tag{3.1}$$

Thus given a possible realization $i_{\pm}(\tau)$, we can generate a typical record an experimentalist would measure by using Eq. (2.2). A typical trajectory for $\psi(\tau)$ is shown in Fig. 1 for a r_{sn} of 570. Here we see, at this value of r_{sn}, the jump in output is clearly visible and occurs at $\tau_d\neq 1$ $(t_d\neq T_1)$.

In the case where the qubit happens to decay early, $\tau_d\ll 1$, the signal s from a qubit initially prepared in the excited state would be almost indistinguishable from that of a qubit initially prepared in the ground state, and even if the measurement apparatus were nearly perfect, almost no information could be extracted. The probability distribution $P_+(s)$ for the measurement signal of an initially excited qubit can be determined analytically with a simple derivation. This will allow a more quantitative discussion of fidelity, and will eventually allow for optimization of integration time, τ_f. The critical difference between the infinite lifetime system described in Sec. II and an actual QND measurement is that s is now a function not only of the dimensionless integration time τ_f, but also the exponentially distributed random relaxation time τ_d.

If the qubit is initially in the excited state, then from Eqs. (2.2), (2.3), and (3.1) a possible realization of $s_{\pm}$ will be

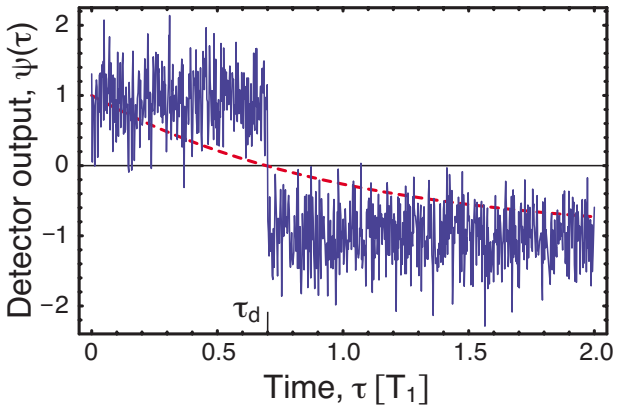

FIG. 1. (Color online) Example detector output as a function of time for a continuous QND measurement with $r_{\mathrm{sn}}=570$ ($d\tau=1\times10^{-4}$), which allows for a measurement fidelity of 99%. The dashed red line corresponds to a large ensemble average of qubit outputs, and decays exponentially with characteristic time T_1. The solid blue line corresponds to the measurement record for a particular single shot. At this value of r_{sn}, the jump in output is clearly visible and occurs at τ_d.

$$s_{\pm}=\tau_f\theta(\tau_d-\tau_f)+(2\tau_d-\tau_f)\theta(\tau_f-\tau_d)+X_G[0,\sigma^2]. \tag{3.2}$$

That is, the probability distribution for s given a realization with a decay at time τ_d is

$$P_+(s|\tau_d)=\frac{1}{\sqrt{2\pi\sigma}}\exp[-(s-\tau_f)^2/2\sigma^2]\theta(\tau_d-\tau_f)+\frac{1}{\sqrt{2\pi\sigma}}\exp\{-[s-(2\tau_d-\tau_f)]^2/2\sigma^2\}\theta(\tau_f-\tau_d), \tag{3.3}$$

and from this one can easily obtain the probability distributions for s by averaging over all possible realizations (decay times). Doing this gives

$$P_+(s)=\frac{1}{\sqrt{2\pi\sigma}}e^{-(s-\tau_f)^2/(2\sigma^2)-\tau_f}+\frac{1}{4}e^{-(s+\tau_f)/2}\times e^{\sigma^2/8}\left\{\mathrm{erf}\left(\frac{\sigma^2-2(s-\tau_f)}{2\sqrt{2}\sigma}\right)-\mathrm{erf}\left(\frac{\sigma^2-2(s+\tau_f)}{2\sqrt{2}\sigma}\right)\right\}. \tag{3.4}$$

Although it does not figure directly into this analysis, it is not difficult to expand this treatment to consider a measurement with finite "demolition" that stimulates both excitation and relaxation of the qubit. In this case, both P_+ and P_- will be non-Gaussian, because the qubit may excite and relax several times during the measurement interval. To calculate the distributions, all we need to do is extend the possible realization to include multiple relaxations and excitations keeping in mind that the relaxation and excitation times are not independent variables: τ_{d_n} must occur before $\tau_{d_{n+1}}$. For stronger or less ideal measurements, it may become necessary to include these extra terms, but for now the demolition is taken to be small compared to the spontaneous relaxation and can be ignored.

The Gaussian first term in Eq. (3.4) is dominant for $\tau_f\ll1$, and $P_+(s)$ is nearly symmetrical to $P_-(s)$. For these fast measurements, there is little chance that the qubit decays during the measurement, and the distributions will be very similar to those of fixed state bits. At some point, the probability that the qubit has relaxed will be large enough that it significantly affects the distributions. At this point, predictions based on the assumption of no relaxation are no longer valid, and the non-Gaussian term in Eq. (3.4) becomes very important. This effect can be seen in the non-Gaussian tail of $P_+(s)$ in the second two time cuts in Fig. 2.

A strongly non-Gaussian P_+ distribution is not required for the fidelity to exhibit a maximum at some finite measurement time. Even though for experiments with $r_{\mathrm{sn}}\approx1$, the non-Gaussian tail of P_+ is not very prominent, the asymmetry between the distributions in both height and width is quite clear. For long enough dimensionless integration times, a qubit initially in the excited state will have probably relaxed relatively early in the measurement, so its mean should be very similar to that of a qubit initially in the ground state, the distributions will be almost identical, and all resolving power will be lost.

B. Optimal box car filter

The behavior of fidelity as a function of integration time for a QND qubit measurement is very different from a measurement of a fixed state qubit that never relaxes. Recall that in the fixed state case, the fidelity eventually converges to one, independent of r_{sn}. We define fidelity as we did for the fixed state case in Eq. (2.5). The difference here is that because the distributions are not necessarily symmetrical, the signal threshold ν_{th} is not always zero. Maximizing F with respect to ν_{th} yields the following implicit equation for ν_{th}

$$P_+(\nu_{\mathrm{th}})=P_-(\nu_{\mathrm{th}}). \tag{3.5}$$

As an aside we note that from this we see that we can write the fidelity (optimized with respect to ν_{th}) in the alternative form

$$F=\frac{1}{2}\int_{-\infty}^{+\infty}ds|P_+(s)-P_-(s)|. \tag{3.6}$$

Despite the complications of finite lifetime, the integrations in Eq. (2.5) can still be carried out analytically to yield

$$F=\frac{1}{2}e^{\sigma^2/8}e^{-(\nu_{\mathrm{th}}+\tau)/2}\left\{\mathrm{erf}\left(\frac{\sigma^2-2(\nu_{\mathrm{th}}-\tau)}{2\sqrt{2}\sigma}\right)-\mathrm{erf}\left(\frac{\sigma^2-2(\nu_{\mathrm{th}}+\tau)}{2\sqrt{2}\sigma}\right)\right\}. \tag{3.7}$$

The fidelity is maximized by numerically solving for ν_{th} such that $P_-(\nu_{\mathrm{th}})=P_+(\nu_{\mathrm{th}})$. Using the correct value of $\nu_{\mathrm{th}}(\tau_f)$, it is straightforward to compute $F(\tau_{\mathrm{f}})$ and then vary τ_f to obtain the optimal value of the integration time.

Roughly speaking, fidelity is a measure of how separate the probability distributions are, ranging between 0 for com-

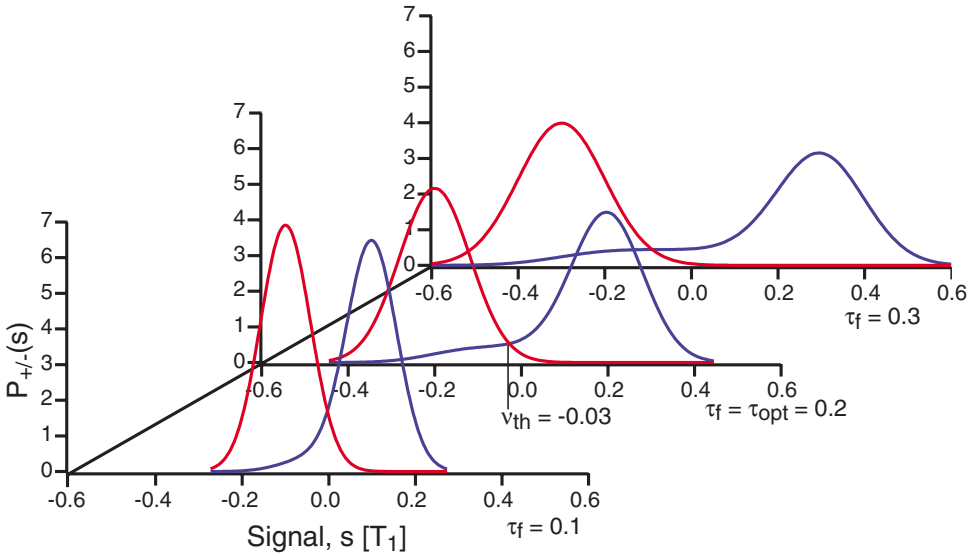

FIG. 2. (Color online) Evolution in time of probability distributions for QND measurement of qubits initialized in the ground (blue) and excited (red) states for the box car linear filter and a $r_{sn}=30$. For short τ_f, the distributions are almost symmetrical because an excited qubit has probably not decayed yet. As τ_f gets longer, the qubit is much more likely to have decayed, and the mean of $P_+(s)$ begins to drift back towards that of $P_-(s)$. At some optimal point in between, $\tau_f=\tau_{opt}$, and if the threshold ν_{th} is chosen so that $P_+(\nu_{th})=P_-(\nu_{th})$, the misidentified tails are minimized, and fidelity is maximized.

plete overlap and 1 for no overlap. Fidelity is limited by detector noise for short times and spontaneous relaxation for long times. For $\tau_f \ll 1$, the probability of a relaxation during the measurement is very low, and the fidelity behaves similarly to the fixed state case: it increases with increasing τ_f. For longer $\tau_f \approx 1$, the qubit is more and more likely to have relaxed during the measurement and the mean of $P_+(s)$ will stop increasing linearly and in the long time limit will actually decrease in time as can be inferred from the decrease in optimal threshold value plotted in Fig. 3(b) (solid line). This implies the existence of some intermediate time $\tau_{opt}(r_{sn})$ that maximizes the fidelity, this is clearly seen in the red solid line of Fig. 3(a) where the fidelity for a $r_{sn}=10$ has a maximum of 0.79 at $\tau_{opt}=0.34$.

To find this time for a given value of r_{sn}, we compute $F(\tau_f)$, then numerically solve $dF(\tau_f)/d\tau_f=0$ for $\tau_f=\tau_{opt}$. The solution, $F_{opt}\equiv F(\tau_{opt})$ is the best possible fidelity for the simple linear box car filter; no improvement can be made from this value without improving the measurement apparatus or the qubit lifetime. This optimal fidelity is only achievable by correctly setting $\tau_f=\tau_{opt}$ and ν_{th}. Any variation of these parameters will reduce the fidelity. It should be pointed out that while the condition $P_-(\nu_{th})=P_+(\nu_{th})$ does maximize the fidelity, it implies that the measurement protocol is biased towards the ground state. That is, if the qubit is prepared in the ground state we are more likely to assign it correctly than if it was prepared in the excited state. An unbiased measurement protocol is obtained by setting ν_{th} such that $\int_{-\infty}^{\nu_{th}} ds\, P_-(s)=\int_{\nu_{th}}^{\infty} ds\, P_+(s)$. Doing this results in a slightly lower optimal fidelity.

Since F_{opt} depends only on r_{sn}, it is possible to first derive the required signal to noise ratio after one lifetime, and then choose the correct measurement time and signal threshold required in order to attain any arbitrary fidelity as shown in

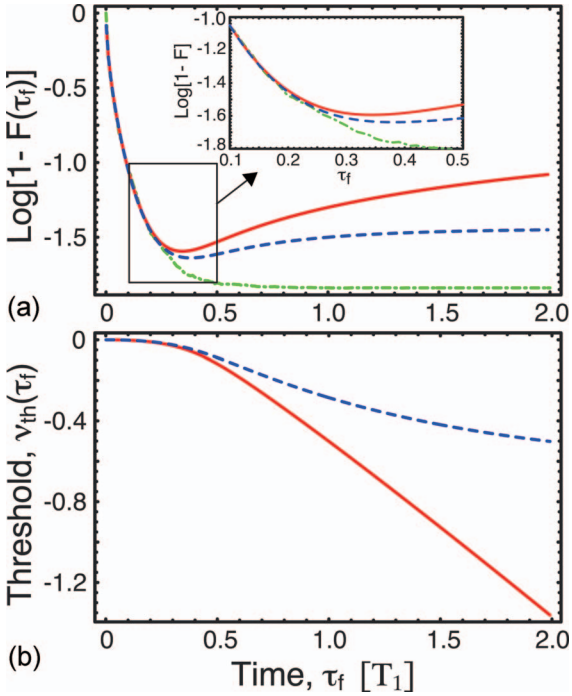

FIG. 3. (Color online) (a) The fidelity F as a function of time τ_f for all measurement protocols. The box car filtered integrated signal is the red (solid) line and the exponential filtered integrated signal is the blue (dashed) line. Here we see that both these schemes have an optimal measurement time and that the latter case is less sensitive to the measurement time. The nonlinear filter is shown by the green (dashed-dotted) line. Here we see that it is clearly better than the other cases and that there is no optimal measurement time. (b) The threshold ν_{th} as a function of time τ_f for both the box car filtered integrated signal (red solid line) and the exponential filtered integrated signal (blue dashed line). In both subplots the r_{sn} after time $\tau_f=1$ is 10 and time is measured in units of T_1.

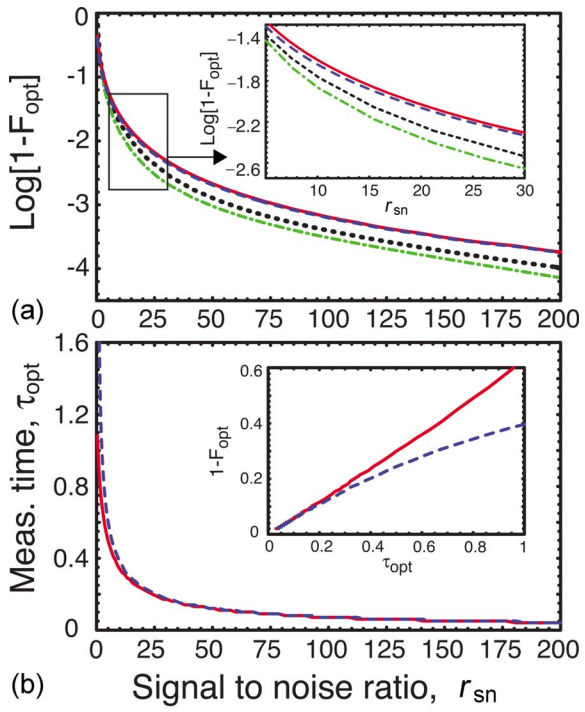

FIG. 4. (Color online) (a) Optimal fidelity F_{opt} and (b) measurement time τ_{opt} as functions of r_{sn}. The inset in (b) shows the optimal fidelity as a function of the measurement time. The red (solid) line is for the box car filter, blue (dashed) is for the exponential filter, black (dotted) is for the optimal linear filter, and green (dashed-dotted) is for the nonlinear filter. Here we see that by using the optimal nonlinear filter we get an improved fidelity in comparison to the simple linear filters. Particular values are shown in Table I.

Fig. 4 [solid line in (a)] along with the optimal measurement time [solid line in (b)]. For example, one standard initial goal is a fidelity of 90%, sufficient to violate Bell's inequalities [36]. As shown in Table I, this fidelity requires a minimum r_{sn} of 30 after time T_1.

The following argument shows how rapidly the required r_{sn} diverges for very high values of fidelity. For large r_{sn}, it is a good approximation to set the threshold $\nu_{\mathrm{th}}=0$ and then the fidelity is approximately

$$F_0 = \exp(-\tau_f/2)\mathrm{erf}(\sqrt{r_{\mathrm{sn}}\tau_f/2}). \tag{3.8}$$

Optimizing this with respect to τ_f and then using the asymptotic form for the error function of large argument yields the following expression for the optimal integration time

$$\tau_{\mathrm{opt}} \approx \frac{2}{r_{\mathrm{sn}}}\left\{x_0 - \frac{1}{2}\ln(x_0)\right\}, \tag{3.9}$$

where $x_0 \equiv \ln[(1+r_{\mathrm{sn}})/\sqrt{\pi}]$.

Approximating the error function in Eq. (3.8) by unity and neglecting $\ln(x_0)$ relative to x_0 leads to the following simple asymptotic form for large r_{sn}:

$$F_0 \sim 1 - \frac{1}{r_{\mathrm{sn}}}\ln\left(\frac{1+r_{\mathrm{sn}}}{\sqrt{\pi}}\right). \tag{3.10}$$

This can be rewritten as in terms of the optimal measurement time as $F_0 \sim 1-\tau_{\mathrm{opt}}/2$. Here we see that to achieve the optimal, the measurement must be completed in a time that decreases linearly with the desired fidelity. The slight deviations form this zeroth order result is shown in the inset of Fig. 4(b). This result is consistent with the intuitive picture that to achieve a fidelity $F=1-\eta$ with $\eta \ll 1$, we must have sufficient r_{sn} to be fooled only by those extremely early decays which occur in time $\tau^* \sim 2\eta$. This set of decays occurs with probability $\sim 2\eta$ and is the main source of the infidelity.

IV. EXPONENTIAL DECAYING LINEAR FILTER

In this section we consider the case when we include an exponential weighting factor in our integrated signal s. This is chosen as this would be the optimal linear filter if our signal was simply a decaying exponential with a random initial amplitude, this can be proven by minimizing our estimate of the amplitude in a least square sense. However, even though our signal on average is of this form, in one particular run it is not. Thus this will not be the optimal linear filter for estimating the initial state of the qubit. For this reason we introduce an integration time τ_{f} and optimize the measurement fidelity over this. That is, the signal s for this filter is given by

$$s = \int_0^{\tau_f} d\tau\, \psi(\tau) e^{-\tau}. \tag{4.1}$$

As in the last section we first determine a possible s given that the qubit started in the excited state. Doing this gives

$$s_{\pm} = \int_0^{\tau_f} d\tau[\theta(\tau_d - \tau) - \theta(\tau - \tau_d)]e^{-\tau} + \sqrt{r_{\mathrm{sn}}^{-1}}\int_0^{\tau_f} dW(\tau)e^{-\tau} \tag{4.2}$$

and by treating the noise integral as simply a linear combination of infinitesimal Gaussian variables gives

$$s_{\pm} = [1 - 2e^{-\tau_d} + e^{-\tau_f}]\theta(\tau_f - \tau_d) + a\,\theta(\tau_d - \tau_f) + X_G[0, \sigma^2], \tag{4.3}$$

where $\sigma = \sqrt{(1-e^{-2\tau_f})/2r_{\mathrm{sn}}}$ and $a = 1-e^{-\tau_f}$. Here we see that unlike before as the measurement time becomes large the variance saturates at $(2r_{\mathrm{sn}})^{-1}$ rather than continuing to increase linearly with time. That is, we have designed our filter such that when all the information about the qubit state has been lost into the T_1 environment the noise in the integrated signal will remain constant.

Following the same procedure as before the excited state distribution is

$$P_+(s) = \frac{1}{4}\left[\mathrm{erf}\left(\frac{a+s}{\sqrt{2}\sigma}\right) + \mathrm{erf}\left(\frac{a-s}{\sqrt{2}\sigma}\right)\right] + \frac{1}{\sqrt{2\pi}\sigma}\exp\left[-\frac{(s-a)^2}{2\sigma^2} - \tau_f\right]. \quad (4.4)$$

Repeating the above for the ground state initial condition gives $s_f = -a + X_G[0,\sigma^2]$ and a ground state distribution of the form

$$P_-(s) = \frac{1}{\sqrt{2\pi}\sigma}\exp\left[-\frac{(s+a)^2}{2\sigma^2}\right]. \quad (4.5)$$

With the above two distributions the fidelity, as before, can be solved analytically and in terms of the ν_{th} is

$$F = \frac{\sigma}{\sqrt{8\pi}}\left(\exp\left[-\frac{(a-\nu_{\mathrm{th}})^2}{2\sigma^2}\right] - \exp\left[-\frac{(a+\nu_{\mathrm{th}})^2}{2\sigma^2}\right]\right) + \frac{(e^{-\tau_f}+1-\nu_{\mathrm{th}})}{4}\left[\mathrm{erf}\left(\frac{a-\nu_{\mathrm{th}}}{\sqrt{2}\sigma}\right) + \mathrm{erf}\left(\frac{a+\nu_{\mathrm{th}}}{\sqrt{2}\sigma}\right)\right].$$

Using the same procedure as before we can numerically determine the ν_{th} which maximizes the fidelity. For a r_{sn} of 10 (in time T_1) the fidelity as a function of measurement time is shown in Fig. 3(a) as a blue dashed line. Here we see as before there is an optimal measurement time. To measure any longer than this time results in a lower fidelity. The optimal fidelity and measurement time are shown in Fig. 4 (blue dashed line) as a function of the r_{sn}. Here we see that by using this filter, the fidelity is slightly better than the simplest case (see Table I for some values), but more importantly the curvature of the fidelity at τ_{opt} is less. This means that this filter is less sensitive to errors in the measurement time. That is, this protocol would be more practical to implement than the simple box car integrated signal of Sec. III.

V. OPTIMAL LINEAR FILTER

In this section we calculate the optimal linear filter for estimating the initial state of the qubit. We define the linear signal s by the relation

$$s = \int_0^\infty k(\tau)\psi(\tau)d\tau, \quad (5.1)$$

where the kernel $k(t)$ is unknown and is determined by maximizing the measurement fidelity. This, as before, is defined as the difference between the probability of us making a correct assignment and an incorrect assignment [Eq. (2.5)]. The assignment criteria we use is again if s is above ν_{th} then we say the qubit was initially up and if it is below ν_{th} then it was down. ν_{th} like $k(t)$ is determined by the maximization procedure which we will describe now.

For an unknown kernel the signal conditioned on the qubit being initially up will be given by

$$s_+ = 2a(\tau_d) - a(\infty) + X_G[0,\sigma^2], \quad (5.2)$$

where

$$a(l) = \int_0^l k(\tau')d\tau', \quad (5.3)$$

$$\sigma = \sqrt{\int_0^\infty k^2(\tau')d\tau'/r_{\mathrm{sn}}}. \quad (5.4)$$

If the qubit was initially in the ground state then the signal would be

$$s_- = -a(\infty) + X_G[0,\sigma^2]. \quad (5.5)$$

From the above equations the excited state and ground state probability distribution for the signal s are

$$P_+(s) = \int_0^\infty \frac{\exp\{-\tau_d - [s-2a(\tau_d)+a(\infty)]^2/2\sigma^2\}}{\sqrt{2\pi\sigma^2}}d\tau_d, \quad (5.6)$$

$$P_-(s) = \frac{\exp\{-[s+a(\infty)]^2/2\sigma^2\}}{\sqrt{2\pi\sigma^2}} \quad (5.7)$$

and by using Eq. (2.5) the fidelity is

$$F = \frac{1}{2}\int_0^\infty e^{-\tau_d}\mathrm{erf}\left(\frac{2a(\tau_d)-a(\infty)-\nu_{\mathrm{th}}}{\sqrt{2}\sigma}\right)d\tau_d - \frac{1}{2}\mathrm{erf}\left(\frac{-a(\infty)-\nu_{\mathrm{th}}}{\sqrt{2}\sigma}\right). \quad (5.8)$$

Maximizing this gives the following set of coupled differential equations

$$d_\tau a(\tau) = k(\tau), \quad (5.9)$$

$$d_\tau k(\tau) = -\exp\{-\tau - 2a(\tau)[a(\tau)-a(\infty)-\nu_{\mathrm{th}}]/\sigma^2\}, \quad (5.10)$$

with the initial conditions $k(0)=1$, $a(0)=0$, and the boundary condition $k(\infty)=0$. It is this latter condition which determines ν_{th}. This system of equations can be solved numerically using a shooting method [37]. The results are shown in Fig. 5 for a r_{sn} of 1.0 and 172. Here we see that for the small r_{sn}, the kernel $k(\tau)$ can be approximated well by $\exp(-\beta\tau)$ where β is a fit parameter that is approximately equal to $1+r_{\mathrm{sn}}/2$. In the large r_{sn} limit the $k(\tau)$ cannot be fit by an exponential. For illustrative purposes the optimal linear filter is compared with the optimal box car linear filter in Fig. 5(b) for a r_{sn} of 172. Here we see that the time when the box car linear filter turns off, is comparable with the time scale of the optimal linear filter.

Numerically solving for $k(\tau)$ for a given σ we can use Eqs. (5.4) and (5.8) to plot the fidelity of the optimal linear filter as a function of the r_{sn}. This is shown in Fig. 4 as a dotted black line and in Table I as column 4. Here we see that the optimal linear filter out performs the other linear filters and is almost as good as the optimal filter (which is nonlinear) and is described in the next section.

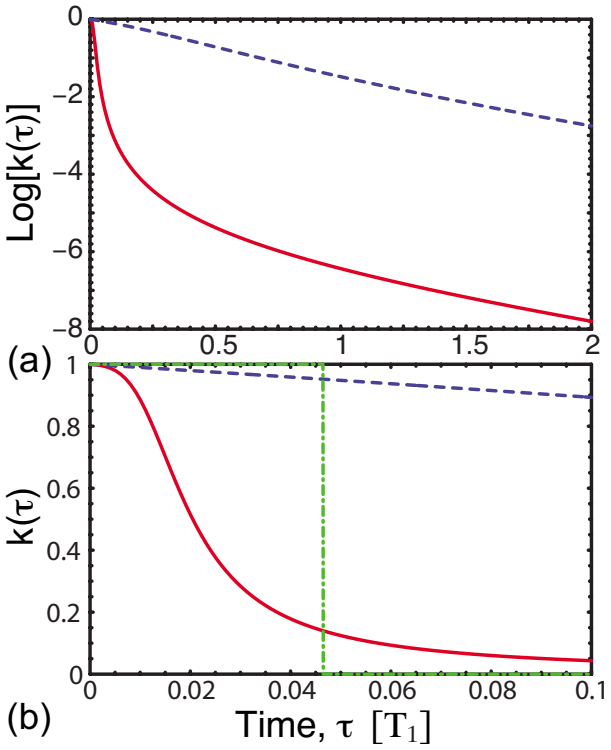

FIG. 5. (Color online) The optimal linear filter for a r_{sn} of 1.0 blue (dashed) and r_{sn} of 172 red (solid) as a function of time. The green (dashed-dotted) line in (b) is the optimal box car linear filter for a r_{sn} of 172 (τ_{opt}=0.046).

VI. OPTIMAL NONLINEAR FILTER

In the previous sections we considered only the case where one looks at or only has access to the integrated signal, $s(\tau)$. Here we assume that we have access to the full record $\Psi=\{\psi(\tau)\}$ and ask how much better can we do with a nonlinear filter. In particular, given this record what is our best guess at the initial state of the qubit. Mathematically, our best guess can be represented by the probability distribution $P(i_0|\Psi)$. This is the probability that the initial condition i_0 is ± 1 given the record, Ψ. As with all probability distributions, this will range from 0 to 1, and the closer it is to one the more we are certain that the qubit was in the initial state $i_0 = \pm 1$. This by definition is the optimal protocol as it is the best estimate of i_0 given the complete set of information available. To find this distribution we use Bayes theorem,

$$P(i_0|\Psi) = \frac{P(\Psi|i_0)P(i_0)}{\sum_{i_0} P(\Psi|i_0)P(i_0)}, \tag{6.1}$$

where $P(i_0)$ is the initial probability distribution and $P(\Psi|i_0)$ is the probability that we would measure record Ψ given that the experiment was initially prepared in state i_0. We will assume that our experiment can prepare unbiased initial states and as such we take $P(i_0 \pm 1)=1/2$. The conditional distribution $P(\Psi|i_0)$ is the probability that we would measure record, Ψ, given that the experiment was initially prepared in state i_0. Thus to calculate $P(i_0|\Psi)$ all we need to do is calculate $P(\Psi|i_0)$. This is the nontrivial step, but can be determined by

$$P(\Psi|i_0) = \sum_p P(\Psi|i_p)P(i_p|i_0), \tag{6.2}$$

where p labels a possible realization of the qubit trajectory. That is, $P(\Psi|i_0)$ can be determined by taking the ensemble average of $P(\Psi|i_p)$ for all possible realizations, i_p [i_p is given by Eq. (3.1) if the qubit is initially in the excited state or $i_p=-1$ if initially in the ground state]. From our simple model for the noise, Eq. (2.1), $P(\Psi|i_p)$ is simply a multiplication of many Gaussians each centered on the instantaneous value of i_p.

For an excited state initial condition, the probability of getting record Ψ will be given by

$$\begin{aligned} P(\Psi|i_0=1) = A\int_0^{\tau_f} d\tau_d e^{-\tau_d} & \\ \times\exp\left[-\int_0^{\tau_d} d\tau[\psi(\tau)-1]^2 r_{sn}/2\right] & \\ \times\exp\left[-\int_{\tau_d}^{\tau_f} d\tau[\psi(\tau)+1]^2 r_{sn}/2\right] & \\ + e^{-\tau_f}\exp\left[-\int_0^{\tau_f} d\tau[\psi(\tau)-1]^2 r_{sn}/2\right]. & \end{aligned} \tag{6.3}$$

Here the first term represents all possible trajectories that have had a decay in time τ_f (the integration time), the second term represents all the trajectories that did not decay in this time, and A is the normalization constant. If the qubit were initially in the ground state then the probability of getting record Ψ will be given by

$$P(\Psi|i_0=-1) = A\exp\left[-\int_0^{\tau_f} d\tau[\psi(\tau)+1]^2 r_{sn}/2\right]. \tag{6.4}$$

Now that we have expressions for $P(\Psi|i_0)$ all that we need to do to get our best estimate of the initial state is to use Eq. (6.1). Doing this gives

$$\begin{aligned} P(i_0=1|\Psi) = \frac{1}{N}\Bigg[\int_0^{\tau_f} d\tau_d e^{-\tau_d}\exp\{[s(\tau_d,0)-s(\tau,\tau_d)]r_{sn}\} & \\ + e^{-\tau_f}\exp[s(\tau_f,0)r_{sn}]\Bigg], & \end{aligned} \tag{6.5}$$

$$P(i_0=-1|\Psi) = \frac{1}{N}\exp[-s(\tau_f,0)r_{sn}], \tag{6.6}$$

where the two time integrated signal $s(\tau,\tau')$ is

$$s(\tau,\tau') = \int_{\tau'}^{\tau} d\tau''\psi(\tau'') \tag{6.7}$$

and the norm is simply

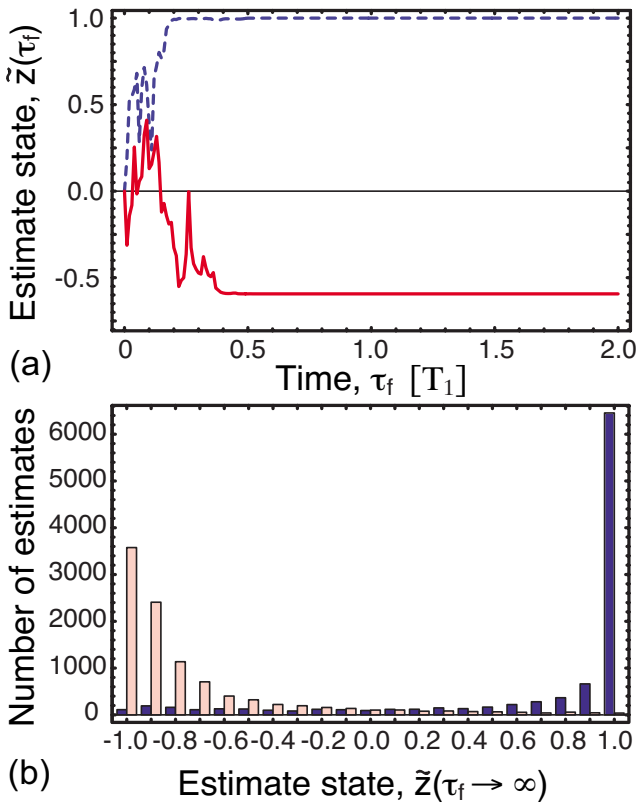

FIG. 6. (Color online) (a) A typical trajectory for the estimated initial condition, $\tilde{z}(\tau_f)$, given a record Ψ which is randomly generated for an excited state initial condition (blue dashed line) and a ground state initial condition (red solid line). (b) A histogram of $\tilde{z}(\tau_f \to \infty)$ for 10^4 trajectories for both an excited state initial condition (dark blue bars column 1) and a ground state initial condition (light red bars column 2). The r_{sn} after $\tau_f=1$ is 10 and time is measured in units of T_1.

$$N = \int_0^{\tau_f} d\tau_d e^{-\tau_d} \exp\{[s(\tau_d,0) - s(\tau,\tau_d)]r_{\mathrm{sn}}\} + e^{-\tau_f}\exp[s(\tau_f,0)r_{\mathrm{sn}}] + \exp[-s(\tau_f,0)r_{\mathrm{sn}}]. \quad (6.8)$$

Here we see that to solve this equation we need to evaluate a double integral over a stochastic process. This is impractical to solve numerically, however, as shown in the Appendix we can easily recast these integrals in terms of two sets of two coupled stochastic differential equations which require similar computational resources to that used with the linear filters.

To show a typical trajectory for this estimated initial condition, we randomly generated records for both an excited and ground state initial condition. Rather then plotting both $P(i_0=1|\Psi)$ and $P(i_0=-1|\Psi)$ we define $\tilde{z}=P(i_0=1|\Psi)-P(i_0=-1|\Psi)$ (this is the estimator that replaces s used in the linear filters), this will range from -1 to 1 and the closer it is to one of these limits, the more certain we are that the initial condition which generated Ψ is this value. The results of this simulation are shown in Fig. 6(a). The solid line corresponds to the case when the initial state was the ground state and the dashed line is for the excited state. Here we see that for this typical trajectory our estimate is fairly good at predicting the real initial condition and we are almost certain for the excited case. However this is only a typical trajectory and to get a better understanding of the predictability of this method we use the same fidelity measure as before, that is we subtract our wrong guesses from our correct guesses. To be more specific, we define the following assignment procedure: if $\tilde{z}>0$ then we assign the qubit as up and if $\tilde{z}<0$ we assign it as down. If $\tilde{z}$ is equal to zero we ignore the result (or flip an unbiased coin to make our decision). Given this assignment criteria we can define the fidelity as

$$F = \lim_{M\to\infty} \frac{1}{2M}\left[\sum_{\tilde{z}_{+1}>0} - \sum_{\tilde{z}_{+1}<0} + \sum_{\tilde{z}_{-1}<0} - \sum_{\tilde{z}_{-1}>0}\right], \quad (6.9)$$

where M is the number of randomly generated Ψ for both +1 and −1 initial conditions. This is shown in Figs. 3(a) and 4(a) as the dashed-dotted line for $M=10^4$ (specific optimal fidelities are listed in Table I). Here we see that the fidelity is always better than the other cases and that there is no optimal measurement time. That is, unlike the box car filter and the exponential linear filter, the fidelity is a nondecreasing function of the integration time.

It should be noted that as in the previous protocols, this is a biased measurement which favors ground state preparations. This can be seen by looking closely at Fig. 6(b). This figure shows a histogram of 10^4 estimates when the system is prepared in the excited state (dark bars, column 1) and the ground state (light bars, column 2) for a $r_{\mathrm{sn}}=10$. If we use our assignment procedure and subtract the wrong guesses from the correct guesses for each prepared initial state we get a fidelity of 0.92 for the ground state and 0.76 for the excited state (an average fidelity of 0.84). This is because when the qubit is prepared in the excited state, rare, early decays will fool the detector.

VII. COMPARISON WITH LATCHING MEASUREMENT

The challenges from qubit relaxation to attaining high fidelity in a continuous measurement also exist in other measurement schemes. For comparison, consider a latching measurement where the qubit state triggers a classical switching event in the measurement apparatus [28–32]. Such a measurement has the advantage that the detector state stays latched for a very long time, so that noise from subsequent amplification stages is completely negligible and the r_{sn} is effectively infinite. We can roughly model this process as an instantaneous measurement with no errors but a finite arming time t_{arm} needed to set up the prelatched state of the detector. We assume that the arming stage occurs after the qubit is prepared but before it is measured. The measurement of a qubit in the excited state will be wrong if the qubit relaxes before the measurement is made. The probability that the qubit relaxes during t_{arm} rises exponentially towards 1, so the fidelity falls exponentially, $F(\tau_{\mathrm{arm}})=e^{-\tau_{\mathrm{arm}}}$. As shown in Table I, τ_{arm} must be slightly smaller than τ_{opt}. Although these times are different in that τ_{arm} is a maximum value whereas τ_{opt} is an optimal value for a given r_{sn}, they provide a valuable comparison between the measurement schemes.

Of course, no latching measurement is truly instantaneous with perfect accuracy in translating the qubit state into latch-

ing events. Moreover, a latching measurement usually induces some mixing of states, so the actual fidelity may be lower than for an equivalent continuous QND measurement. Both measurement schemes have their own strengths and weaknesses, but in either case, qubit decay can be a significant limiting factor on the fidelity.

VIII. CONCLUSION

We have examined the effect of qubit relaxation on the estimation of the qubit initial state (excited or ground) using a continuous-in-time noisy quantum nondemolition measurement for four different measurement protocols. In these protocols the measurement results are integrated with a box car linear filter, an exponentially decaying filter, an optimal linear filter and a nonlinear Bayesian filter which by definition is the optimal theoretical filter. We found that in all these protocols there exists a theoretical limit on the measurement fidelity. The determining factor of this limit is the signal to noise ratio of the measurement. Our results are summarized in Table I where we see that the non-linear filter reaches the same fidelity as the linear filters even for substantially lower required signal to noise ratio. Lastly we compare the continuous quantum nondemolition results with latching measurements and found that there is a quantitatively different but qualitatively similar limit on the fidelity of latching measurements also due to relaxation. The signal to noise ratio required to do successful qubit single shot quantum nondemolition measurements should be attainable in the near future, and there is no fundamental reason why significantly higher fidelity measurements cannot be performed.

ACKNOWLEDGMENTS

We thank Michel Devoret, Isaac Chuang, Alexandre Blais, Jens Koch, Andrew Houck, and David Schuster for discussions. This work was supported in part by NSA under ARO Contract No. W911NF-05-1-0365, and the NSF under Grants ITR-0325580, DMR-0342157, and DMR-0603369, and the W. M. Keck Foundation.

APPENDIX: NUMERICAL PROCEDURE USED BY THE OPTIMAL NONLINEAR FILTER

In this appendix we present the method used to simulate the optimal nonlinear filter. This filter requires simulating Eqs. (6.5) and (6.6) which contains a double integral over a stochastic process $\psi(\tau)$. This is not practical numerically and a much better method can be implemented by deriving a set of coupled stochastic differential equations. To do this we start by rewriting Eqs. (6.5) and (6.6) as

$$P(i_0 = 1|\Psi) = \frac{\bar{P}_{+1,\psi}}{\bar{P}_{-1,\psi} + \bar{P}_{+1,\psi}}, \tag{A1}$$

$$P(i_0 = -1|\Psi) = \frac{\bar{P}_{-1,\psi}}{\bar{P}_{-1,\psi} + \bar{P}_{+1,\psi}}, \tag{A2}$$

where

$$\bar{P}_{+1,\psi} = e^{-\tau_f}\exp[s(\tau_f,0)r_{\mathrm{sn}}] + \int_0^{\tau_f} d\tau_d e^{-\tau_d} \times \exp\{[s(\tau_d,0) - s(\tau_f,\tau_d)]r_{\mathrm{sn}}\}, \tag{A3}$$

$$\bar{P}_{-1,\psi} = \exp[-s(\tau_f,0)r_{\mathrm{sn}}], \tag{A4}$$

and the signal $s(\tau,\tau')$ is defined in Eq. (6.7). We first differentiate $\bar{P}_{+1,\psi}$ with respect to τ_f and by defining

$$\lambda_{+1,\psi} = e^{-\tau_f}\exp[s(\tau_f,0)r_{\mathrm{sn}}] - \int_0^{\tau_f} d\tau_d e^{-\tau_d} \times \exp\{[s(\tau_d,0) - s(\tau_f,\tau_d)]r_{\mathrm{sn}}\}, \tag{A5}$$

we get the following set of coupled stochastic differential equations

$$\frac{d}{d\tau_f}\bar{P}_{+1,\psi} = r_{\mathrm{sn}}\psi(\tau)\lambda_{+1,\psi}, \tag{A6}$$

$$\frac{d}{d\tau_f}\lambda_{+1,\psi} = r_{\mathrm{sn}}\psi(\tau)\bar{P}_{+1,\psi} - (\lambda_{+1,\psi} + \bar{P}_{+1,\psi}), \tag{A7}$$

and the initial conditions $\lambda_{+1,\psi}=1$ and $\bar{P}_{+1,\psi}=1$. If we use Eq. (A4) the two additional coupled equations are

$$\frac{d}{d\tau_f}\bar{P}_{-1,\psi} = r_{\mathrm{sn}}\psi(\tau)\lambda_{-1,\psi}, \tag{A8}$$

$$\frac{d}{d\tau_f}\lambda_{-1,\psi} = r_{\mathrm{sn}}\psi(\tau)\bar{P}_{-1,\psi}, \tag{A9}$$

with initial conditions $\lambda_{-1,\psi}=-1$ and $\bar{P}_{-1,\psi}=1$. Note that since there is no relaxation, we do not need to have two equations for the ground state, we can just use $d_{\tau_f}\bar{P}_{-1,\psi} = -r_{\mathrm{sn}}\psi(\tau)\bar{P}_{-1,\psi}$, but to keep the problem symmetrical we have decided to leave both equations in. This makes it easier to extend the theory to cases where upward jumps are possible.

Thus to simulate Eqs. (6.5) and (6.6) we simply solve the above two sets of two coupled differential equations and then combine them using Eqs. (A1) and (A2). Note an equivalent derivation of these equations can be made by using the Kushner-Stratonovich equation [38] and then simply using Bayes theorem to invert these equations for estimating unknown parameters [39].

[1] H. J. Carmichael, *An Open Systems Approach to Quantum Optics* (Springer-Verlag, Berlin, 1993).
[2] Y. Makhlin, G. Schon, and A. Shnirman, Phys. Rev. Lett. **85**, 4578 (2000).
[3] A. N. Korotkov, Phys. Rev. B **63**, 115403 (2001).
[4] Y. Makhlin, G. Schoen, and A. Shnirman, Rev. Mod. Phys. **73**, 357 (2001).
[5] A. N. Korotkov and D. V. Averin, Phys. Rev. B **64**, 165310 (2001).
[6] H.-S. Goan, G. J. Milburn, H. M. Wiseman, and H. B. Sun, Phys. Rev. B **63**, 125326 (2001).
[7] Asher Peres, *Quantum Theory: Concepts and Methods* (Kluwer Academic Publishers, Dordrecht, Netherlands, 1993).
[8] W. Nagourney, J. Sandberg, and H. Dehmelt, Phys. Rev. Lett. **56**, 2797 (1986).
[9] T. Sauter, W. Neuhauser, R. Blatt, and P. E. Toschek, Phys. Rev. Lett. **57**, 1696 (1986).
[10] D. J. Wineland, C. Monroe, W. M. Itano, D. Leibfried, B. King, and D. M. Meekhof, J. Res. Natl. Inst. Stand. Technol. **103**, 259 (1998).
[11] D. I. Schuster, A. Wallraff, A. Blais, L. Frunzio, R. S. Huang, J. Majer, S. M. Girvin, and R. J. Schoelkopf, Phys. Rev. Lett. **94**, 123602 (2005).
[12] J. Gambetta, A. Blais, D. I. Schuster, A. Wallraff, L. Frunzio, J. Majer, M. H. Devoret, S. M. Girvin, and R. J. Schoelkopf, Phys. Rev. A **74**, 042318 (2006).
[13] M. Nielsen and I. Chuang, *Quantum Computation and Quantum Information* (Cambridge University Press, Cambridge, UK, 2000).
[14] B. Kane, Nature (London) **393**, 133 (1998).
[15] C. van der Wal, A. ter Haar, F. Wilhelm, R. Schouten, C. Harmans, T. Orlando, S. Lloyd, and J. Mooij, Science, **290**, 773 (2000).
[16] R. Vrijen, E. Yablonovitch, K. Wang, H. W. Jiang, A. Balandin, V. Roychowdhury, T. Mor, and D. DiVincenzo, Phys. Rev. A **62**, 012306 (2000).
[17] D. Vion, A. Aassime, A. Cottet, P. Joyez, H. Pothier, C. Urbina, D. Esteve, and M. Devoret, Science **296**, 886 (2002).
[18] I. Chiorescu, Y. Nakamura, C. Harmans, and J. Mooij, Science **299**, 1869 (2003).
[19] O. Astafiev, Y. A. Pashkin, T. Yamamoto, Y. Nakamura, and J. S. Tsai, Phys. Rev. B **69**, 180507(R) (2004).
[20] C. Langer, R. Ozeri, J. D. Jost, J. Chiaverini, B. DeMarco, A. Ben-Kish, R. B. Blakestad, J. Britton, D. B. Hume, W. M. Itano, D. Leibfried, R. Reichle, T. Rosenband, T. Schaetz, P. O. Schmidt, and D. J. Wineland, Phys. Rev. Lett. **95**, 060502 (2005).
[21] A. Blais, R.-S. Huang, A. Wallraff, S. M. Girvin, and R. J. Schoelkopf, Phys. Rev. A **69**, 062320 (2004).
[22] A. Wallraff, D. I. Schuster, A. Blais, L. Frunzio, R. S. Huang, J. Majer, S. Kumar, S. M. Girvin, and R. J. Schoelkopf, Nature (London) **431**, 162 (2004).
[23] A. Wallraff, D. I. Schuster, A. Blais, L. Frunzio, J. Majer, M. H. Devoret, S. M. Girvin, and R. J. Schoelkopf, Phys. Rev. Lett. **95**, 060501 (2005).
[24] D. DiVincenzo, G. Burkard, D. Loss, and E. Sukhorukov, in *Quantum Mesoscopic Phenomena and Mesoscopic Devices in Microelectronics*, edited by I. Kulik and R. Ellialtioglu (NATO Advanced Study Institute, Turkey, 1999), e-print arXiv:cond-mat/9911245.
[25] H. A. Engel, V. N. Golovach, D. Loss, L. M. K. Vandersypen, J. M. Elzerman, R. Hanson, and L. P. Kouwenhoven, Phys. Rev. Lett. **93**, 106804 (2004).
[26] K. B. Cooper, M. Steffen, R. McDermott, R. W. Simmonds, S. Oh, D. A. Hite, D. P. Pappas, and J. M. Martinis, Phys. Rev. Lett. **93**, 180401 (2004).
[27] P. Bertet, I. Chiorescu, K. Semba, C. J. P. M. Harmans, and J. E. Mooij, Phys. Rev. B **70**, 100501(R) (2004).
[28] J. M. Martinis, S. Nam, J. Aumentado, and C. Urbina, Phys. Rev. Lett. **89**, 117901 (2002).
[29] N. Katz, M. Ansmann, R. C. Bialczak, E. Lucero, R. McDermott, M. Neeley, M. Steffen, E. M. Weig, A. N. Cleland, J. M. Martinis, and A. N. Korotkov, Science **312**, 1498 (2006).
[30] I. Siddiqi, R. Vijay, F. Pierre, C. M. Wilson, M. Metcalfe, C. Rigetti, L. Frunzio, and M. H. Devoret, Phys. Rev. Lett. **93**, 207002 (2004).
[31] I. Siddiqi, R. Vijay, F. Pierre, C. M. Wilson, L. Frunzio, M. Metcalfe, C. Rigetti, R. J. Schoelkopf, M. H. Devoret, D. Vion, and D. Esteve, Phys. Rev. Lett. **94**, 027005 (2005).
[32] I. Siddiqi, R. Vijay, M. Metcalfe, E. Boaknin, L. Frunzio, R. J. Schoelkopf, and M. H. Devoret, Phys. Rev. B **73**, 054510 (2006).
[33] T. Duty, D. Gunnarsson, K. Bladh, and P. Delsing, Phys. Rev. B **69**, 140503(R) (2004).
[34] K. W. Lehnert, B. A. Turek, K. Bladh, L. F. Spietz, D. Gunnarsson, P. Delsing, and R. J. Schoelkopf, Phys. Rev. Lett. **91**, 106801 (2003).
[35] C. Gardiner, *Handbook of Stochastic Methods: for Physics, Chemistry and the Natural Science* (Springer, Berlin, 1985).
[36] T. Jennewein, G. Weihs, J. W. Pan, and A. Zeilinger, Phys. Rev. Lett. **88**, 017903 (2001).
[37] W. H. Press, S. A. Teukolsky, W. T. Vetterling, and B. P. Flannery, *Numerical Recipes in C++* (Cambridge University Press, Cambridge, UK, 2002).
[38] T. P. McGarty, *Stochastic Systems and State Estimation* (John Wiley & Sons, New York, 1974).
[39] J. Gambetta and H. M. Wiseman, Phys. Rev. A **64**, 042105 (2001).